Christian Joachim
Editor

Atomic Scale Interconnection Machines

Proceedings of the 1st AtMol European Workshop Singapore 28th–29th June 2011

Springer

Christian Joachim
CNRS
GNS
Rue J. Marvig 29
31055 Toulouse Cedex
France

ISSN 2193-9691
ISBN 978-3-642-28171-6
DOI 10.1007/978-3-642-28172-3
Springer Heidelberg New York Dordrecht London

e-ISSN 2193-9705
e-ISBN 978-3-642-28172-3

Library of Congress Control Number: 2012933100

Printed on acid-free paper

Springer is part of Springer Science+Business Media (www.springer.com)

Preface

Atom Technology is essential for the construction and study of dangling bond logic circuits, single molecule logic gates and for single molecule mechanical machineries. One of the first instruments urgently required for experimental work at the atomic scale is a machine with an atomic scale precision offering the possibility to exchange information and energy with single and well-identified molecule machineries. These nano-communication-like machines must also offer dedicated navigation abilities for the interconnection probes to be positioned on the device with atomic scale precision. As a result of this need for such instruments in many laboratories around the world, the Integrated European Project AtMol decided to organize its first biannual workshop on the topic of "Atomic Scale Interconnection Machines". Fully supported by the ICT-FET of INFSO at the European level, AtMol was launched on 1 January 2011, for 4 years, with the objective to construct the first ever complete molecular chip. This Atomic Scale Interconnection Machines workshop event took place at IMRE in June 2011, where IMRE-A*STAR is the AtMol partner based in Singapore.

This first volume of the new Springer Series "Advances in Atom and Single Molecule Machines" compiles all the contributions presented during this workshop. The workshop was the first to involve a large number of laboratories from all around the world working on the construction, the development or usage of atomic scale interconnection machines. All the possible categories of these very often large, ultra high vacuum (UHV) instruments were presented by different communities, from academics to high-tech companies who develop the new hardware, or control the software of these machines. Examples include, multiple LT-UHV STM systems, multiple LT-NC-AFM systems, optical navigation, SEM navigation and even the first machines demonstrating single atom and molecular manipulation capability together with the nano-communication setup.

The organizing committee of the first workshop of the AtMol series is happy to thank the ICT-FET division of European Commission and A*STAR of Singapore for the financial support to organize this first workshop. We are expecting to

launch a quite unique series of events to boost Atom Technologies from a practical point of view. The upcoming workshops in the AtMol series will be announced on the www.atmol.eu official web site. The organizing committee also wishes to thank all the participants in Singapore for a very dynamic workshop.

For the organizing committee
C. Joachim

Contents

Nanometer-Scale Four-Point Probe Resistance Measurements of Individual Nanowires by Four-Tip STM

S. Hasegawa, T. Hirahara, Y. Kitaoka, S. Yoshimoto, T. Tono and T. Ohba

Abstract We present a review of our recent results about transport properties of nanowires measured by a four-tip scanning tunneling microscope (STM) installed with metal-coated carbon nanotube (CNT) tips. We first present our custom-made apparatus (with UNISOKU Co.) as well as CNT tips, and then some case studies with two different samples, Co-silicide nanowires self-assembled on Si(110) surface and Cu nanowires made by damascene processes used in LSI industry. It is shown that the four-tip STM with CNT tips is versatile and powerful for measuring the conductivity of individual nanostructures.

1 Introduction

Conductivity measurements in sub-micron or nanometer scale are of great interest in nanoscience and nanotechnology. For example, nanoelectronics such as semiconductor devices requires low and stable electrical resistance of interconnects to maintain device performance. Several kinds of methods to measure the conductivity at nanoscales have been developed including fixed electrodes made by microlithography techniques. A method which adopts tips of scanning tunneling

S. Hasegawa (✉) · T. Hirahara · Y. Kitaoka · S. Yoshimoto · T. Tono
Department of Physics, School of Science, University of Tokyo, 7-3-1, Hongo, Bunkyo-ku, Tokyo 113-0033, Japan
e-mail: shuji@surface.phys.s.u-tokyo.ac.jp

T. Ohba
School of Engineering, University of Tokyo, Tokyo 113-0033, Japan

S. Yoshimoto
Institute of Solid State Physics, University of Tokyo, Kashiwa 277-8581, Japan

C. Joachim (ed.), *Atomic Scale Interconnection Machines*, Advances in Atom and Single Molecule Machines, DOI: 10.1007/978-3-642-28172-3_12,

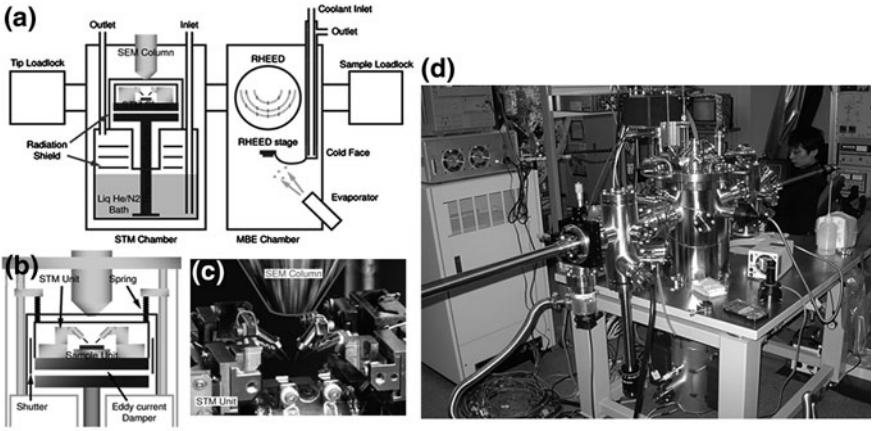

Fig. 1 Schematic drawings of the whole system of low-temperature four-tip STM (**a**) and around the STM stage (**b**) [14]. **c** A close-up photo of the STM stage without radiation shields. **d** The photo of the whole system

microscope (STM) as electrodes, however, has great advantages in positioning of the probes in arbitrary configurations as well as in high spatial resolution of measurements. But single-tip STM is not enough for versatile measurements of transport properties at various kinds of nanostructures: we need source, drain, and gate electrodes. For this reason, several groups [1–10] including companies [11] and our group [12–14] have developed four-tip STM, in which four independent STM tips are operated in an organic manner with aid of a SEM or optical one, and they are used as electrodes for microscopic two- or four-point probe (μ4PP) conductance measurements. In this article, we show our apparatuses including installation of carbon nanotube tips [15–17] and some results of resistance measurements of nanowires obtained in our group.

2 Four-Tip STM System

Figures 1a, b show schematic drawings of our new version of four-tip STM system [14], consisting of a main (STM) chamber, a sample preparation molecular beam epitaxy (MBE) chamber, and two load-lock chambers for sample and tip exchanges, all of which are UHV compatible. The STM tips can be installed into the main chamber from the tip load-lock chamber where a hot W filament is installed for out-gassing of the tips. The sample is introduced from the MBE chamber where cleaning of the sample, deposition of materials and reflection-high-energy electron diffraction (RHEED) observation can be done. The sample can be heated by direct current heating and cooled down to about 30 K by continuous-flow type cryostat in the MBE chamber. These capabilities are necessary for

preparing aimed surface superstructures, epitaxial thin films, nanodots, nanowires, and for making in situ measurements.

The STM stage is mounted on the thermal conducting Cu rod which is soaked in the coolant of the bath cryostat below. The STM stage including the sample and four sets of actuator units is wholly surrounded with two-fold radiation shields and movable shutters. The photo of Fig. 1c is the stage without the radiation shields, and Fig. 1d shows the whole system. The sample and tips can be cooled down to 7 K and can be kept for 23 h with liquid He as coolant. In the case of liquid N_2, the minimum temperature is 80 K and the preserved time is longer than three days.

The SEM column (APCO Mini-EOC) is mounted above the STM stage. The working distance of SEM is about 25 mm. The electron beam is irradiated from SEM column through a 1 mm diameter hole in the radiation shields. A multi-channel plate for the secondary electron detection for SEM imaging is placed on the inside wall the outer shield. The SEM image is obtained from the secondary electron signal or beam induced current signal electron-beam-induced current image (EBIC). The resolution of the SEM is about 20 nm for both signals.

A spring vibration isolator and an eddy-current damper are built between the thermal conductor and the STM stage to avoid vibration of STM stage. The spring isolator decoupled the STM stage from other components. However, during SEM observation, tip/sample exchanges, and cooling the stage, the STM stage is fixed to the thermal conductor (Cu rod) and therefore the isolator and damper are disabled. When we fix the STM stage, the Cu plate works as a thermal conductor and enlarges the contact area for good thermal connection. When we float the STM stage by the springs, this plate makes eddy-current damper. Since alternative arrangements of the small magnets make closed magnetic paths, the magnetization does not affect the SEM beam.

Four sets of tip actuator units are mounted at the corner of the square STM stage, and a sample actuator unit is placed at the center. The actuator units consist of stacked piezo ceramics supported by sapphire plates. For fine positioning or scanning in nanometer or sub-nanometer range, tips and samples are driven by conventional piezoelectric effect of the ceramics by DC voltage. The maximum positioning range by this method is about 2 μm to each direction. For coarse positioning, the actuators are driven by stick–slip mechanism in 5 mm travel distance in XY directions and 2.5 mm in Z direction at accuracy of about 100 nm. In addition to these three- or two-dimensional-motion actuators, the tip actuators also contain small piezo ceramics near the tips for fast STM feedback.

Figure 2 shows a series of SEM images of the four tips arranged in various configurations [12, 13, 18]. The tips are chemically etched W wires. The probe spacing can be changed from 1 mm to ca. 200 nm in Figs. 2a–c. They can be arranged on a line equidistantly (linear μ4PP method) (c, d) in arbitrary directions, or in square arrangement (square-μ4PP method) Figs. 2e–h. The square can be rotated with respect to the sample surface (rotational square-μ4PP method) by re-positioning each tip under computer control. This is useful to measure anisotropic surface conductivity in which the conductivity is different depending on the crystal orientation.

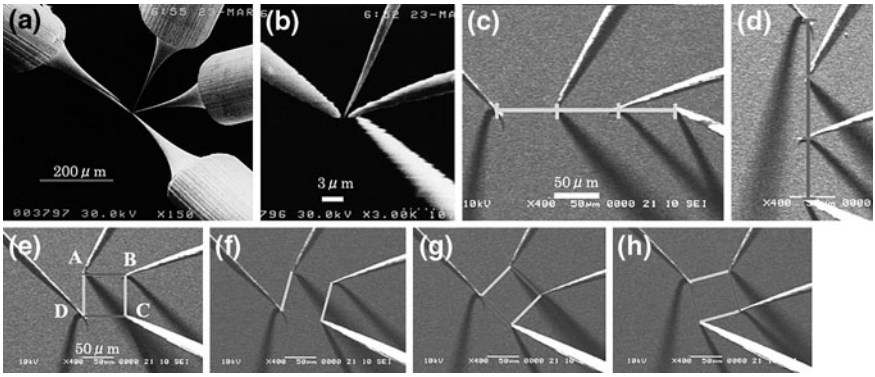

Fig. 2 SEM images of the four W tips in various arrangements in the four-tip STM [12, 13, 18]

3 Metal-Coated Carbon Nanotube Tips

An important issue for the four-tip STM is the probe spacing; the probe spacing should be in the order of 10 nm to measure various kinds of nanostructures. At the present the minimum probe spacing in the multi-tip STM is approximately 100 nm when W tips are used. This is due to the radius of tip apex of electrochemically etched W tips. This probe spacing is not small enough for observing ballistic transport and quantum interference effects because the coherence length of conduction carriers is shorter than 100 nm in many cases. For this reason, continuous efforts are made to shorten the probe spacing down to ca. 10 nm. To make the probe spacing shorter, carbon nanotube tips have been developed in which a carbon nanotube is glued at the end of W tip [19–22]. Since the radius of the (multi-walled) carbon nanotubes is usually ca. 10 nm and the aspect ratio is much higher than usual W tips, two carbon nanotube tips can be brought together into approximately 10 nm spacing. Another feature of the carbon nanotube tip is its mechanical flexibility which can reduce damage to delicate samples such as organic and biological molecules, and make the tips withstand numerous direct contacts to the samples. These properties are quite convenient for the transport measurements by multi-tip STM at nanometer scales. However, there have been problems in the carbon nanotube tips; high contact resistance between the supporting metal tip and the attached carbon nanotube strongly disturbs electron transport at the STM/STS measurements. Moreover, adsorbates contained in the carbon nanotube degrade the surface cleanness of the specimen under STM operation.

A novel technique for overcoming these difficulties has been developed; the carbon nanotube together with the supporting metal tip is wholly coated with a thin metal layer [15]. Figures 3a,b show TEM images of a W-coated carbon nanotube tip glued on a W supporting tip. The W layer of ca. 3 nm thick was deposited by pulsed laser deposition (PLD) method. The W layer fully covers the tip even at the

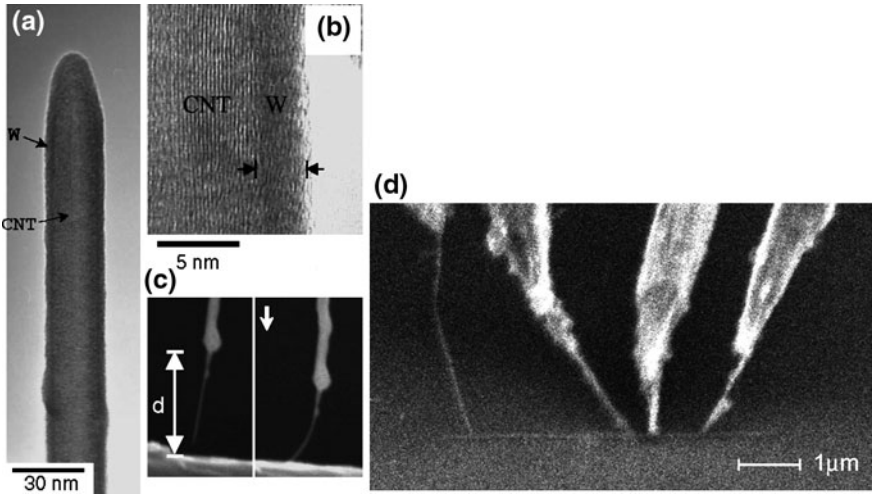

Fig. 3 **a** TEM image and **b** high-resolution TEM image of a W-coated carbon nanotube tip coated by pulsed laser deposition method. **c** SEM images of the W-coated carbon nanotube tip, directly contacting to a sample surface. Reproduced from Ref. [15]. **d** A SEM image showing four carbon nanotube tips contacting a Co-silicide nanowire grown on a Si substrate [23]

end. Figure 3c shows flexibility and robustness of the W-coated carbon nanotube tip upon the direct contact to a sample surface. Figure 3d is a SEM image showing four CNT tips contacting a Co-silicide nanowire grown on a Si substrate [23]. We have also confirmed that the electrical resistance at the glued point between the carbon nanotube and supporting W tip is stably reduced by the metal coating; especially PtIr coating is the most efficient for this purpose [16]. Atomic-resolution STM imaging and STS spectra were acquired with the W-coated carbon nanotube tip at the first attempt [15]. With this metal-coated carbon nanotube tips, we have succeeded in bringing the two tips together into less than 30 nm [17, 23, 24]. Since the resolution of SEM is not enough for observing a smaller probe spacing, we believe that the minimum spacing can be reduced to ca. 20 nm, similar to the diameter of CNT itself.

4 Measuring Co-Silicide Nanowires

$CoSi_2$ nanowires are known to grow self-assembly by depositing high-purity cobalt on a Si(110) clean surface held at 750–850°C in UHV, as shown in Figs. 4a–c [25]. The nanowires become longer and thinner with lowering the substrate temperature during the Co deposition. The wires are single-crystalline, half of which is embedded in the Si substrate as observed by a cross-sectional TEM image of Fig. 4d [25]. The $CoSi_2$ is known to be highly conductive metallic

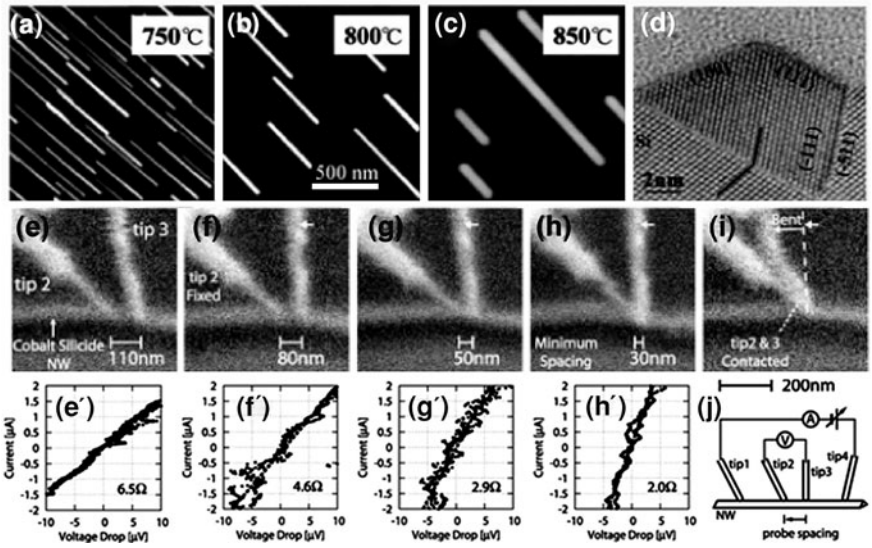

Fig. 4 **a**–**c** Atomic force microscopy images of $CoSi_2$ nanowires formed by depositing Co on the heated Si(110) substrate at different temperatures reproduced [25]. **d** A cross-sectional TEM image of the nanowire from Ref. [25]. **e**–**h** SEM images of the inner pair of CNT tips (tip 2 and tip 3 in (j)), with different probe spacings, contacting one of the nanowires during the resistance measurements in the four-tip STM [23]. The current probes (tip 1 and tip 4) are about 1 μm away from these voltage probes. **e′**–**h′** Four-terminal current–voltage curves measured at the tip configuration shown in **e**–**h**, respectively [23]. The four-terminal resistance R_4t decreased with reducing the probe spacing. **i** The voltage probes contacted each other, and the tip 3 was bent. **j** A schematic showing the four-terminal current–voltage measurements

and its resistivity is 31 ± 9 μΩ cm for the nanowire [26] and ∼15 μΩ cm for the films [27] at 300 K.

As shown in Fig. 3d, the four CNT tips were made contact onto one of the nanowires under SEM observation. The tips were made approach beyond the point of tunneling until the contact resistances became less than 1 MΩ, corresponding to direct contact. At the current–voltage (I–V) measurement, the STM feedback loops were cut. Even if the tip physically contacted the NW, the contact resistance between the tip and sample was higher than 50 kΩ. It was difficult to reduce this resistance because of the nanometer-sized contact area. This is much larger than the resistance of the nanowire itself, which is less than 1 kΩ with probe spacing smaller than 1 μm [26]. Therefore, by two-terminal I–V measurements, the resistance did not depend on the probe spacing due to the large contact resistance at the probe contacts: four-point measurements are indispensable at nanometer scale.

Four-terminal I–V measurements were done by sweeping the bias voltage between tip 1 and tip 4 with recording the current I and the voltage drop V between tip 2 and tip 3, with changing the spacing between tip 2 and tip 3 as shown in Figs. 4e–h. The SEM beam was stopped at the I–V measurements to avoid possible influence on

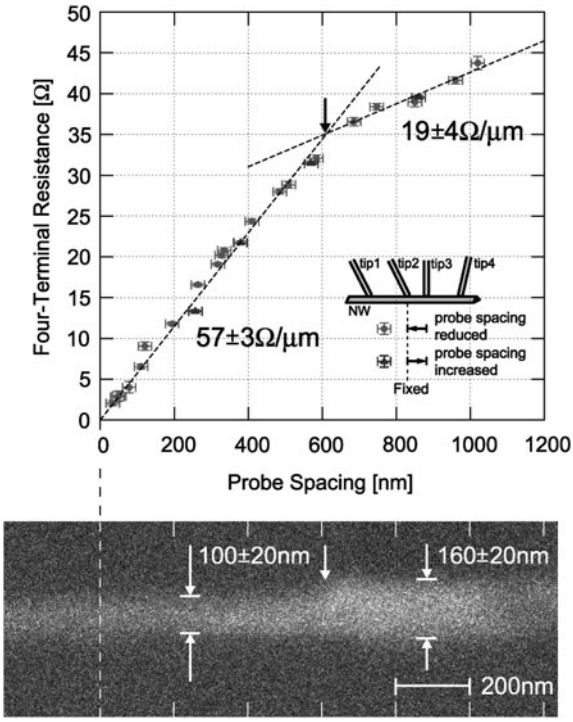

Fig. 5 The measured four-terminal resistance R_4t as a function of the spacing between the voltage probes, and SEM image of the nanowire under measurement (*top view*). The *black arrow* around 600 nm in the graph and the *white arrow* in the SEM image indicate the position where the nanowire width changes, resulting in a change of the resistivity [23]

the resistance caused by high-energy electron beam (10 kV). Figures 4e–h show a series of SEM images around the voltage probes (tip 2 and tip 3) touching on the nanowire, and corresponding four-terminal I–V curves are shown in (e′–h′). We reduced the probe spacing between the voltage probes during taking the I–V characteristics. The positions of the two current probes (tip 1 and tip 4) and one of the voltage probes (tip 2) were fixed in the measurements, and only tip 3 was shifted. All I–V curves were linear. The four-terminal resistance $R_4t = \mathrm{dV/dI}$ around $\mathrm{I} = 0$ decreased with shortening the probe spacing. They are several Ω, much smaller than the contact resistance. A voltage amplifier was introduced at the STM pre-amplifiers to detect small voltage drops resulted from the small resistance. Finally tip 3 bent as shown in Fig. 4i, and R_4t became 0 Ω because of direct contact between the voltage probes. The minimum probe spacing achieved here was 30 ± 20 nm as shown in Fig. 4h. This was limited by the diameter of the CNT tip apex we used, 30 nm (20 nm diameter of CNT + 5 nm thick PtIr layer). The error bar in the probe spacing is determined by the radii of the apexes in tip 2 and tip 3.

We plot the measured four-terminal resistance R_4t as a function of the spacing between the contact points of the voltage probes on the nanowire in Fig. 5. The linear proportional relation in the range 30–600 nm means diffusive transport, and the fit line gives one-dimensional resistivity $\rho_{1D} = 57 \pm 3$ Ω/μm. By extrapolating the data points, there seems to be no residual resistance at zero probe

Table 1 Probe spacing L dependence of the four-terminal resistance R_4t in various conduction mechanisms

Conduction mechanism	1D Ohmic	2D Ohmic	3D Ohmic	1D strong localization	1D weak localization	Ballistic
L-dependence of R_4t	$\propto L^1$	$\propto L^0$ (constant)	$\propto L^{-1}$	$\propto \exp\left(\frac{L}{L_0}\right)$	$\propto \frac{L}{L_0-L}$	$\propto L^0$ (with fluctuation)

L_0 is the localization length

spacing, which is owing to the four-point probe configuration. The gradient decreased to 19 ± 4 Ω/μm above 600 nm probe spacing. This is due to an increase of the nanowire width from 100 ± 20 to 160 ± 20 nm as shown in the SEM image in Fig. 5. By checking the reproducibility we found that the physical contacts of the CNT tips did not cause any significant damage to the nanowire.

We now discuss the transport property of the NW. Table 1 shows a list of the probe spacing L dependence of the four-terminal resistance in various conduction mechanism. The probe spacing dependence of resistance in $CoSi_2$ nanowire showed a linear one-dimensional Ohmic feature ($R_4t \propto$ L). This behavior is due to a one-dimensional conduction path through the nanowire without leakage of current to the underlying three-dimensional substrate or to the two-dimensional substrate surface. This is because a Schottky barrier between the nanowire and the Si substrate confines the current [26]. The mean free path of the electrons in $CoSi_2$ is around 6 nm at room temperature [28], which is much smaller than the width and height of our nanowire as well as the probe spacing. Therefore, our result of diffusive conduction is reasonable. The three-dimensional resistivity of the nanowire can be calculated. The width of the nanowire is determined by SEM image, and the height can be determined by the transmission electron microscope image [25]. We obtain the three-dimensional resistivity 22 ± 4 μΩ cm. In the same way, we obtain 19 ± 4 μΩ cm for the region larger than 600 nm. These values are comparable to the previous results (31 ± 9 μΩ cm) in which similar $CoSi_2$ NWs were measured with W tips in larger probe spacing range [26].

In the ballistic transport regime, two-terminal and four-terminal resistances (R_2t and R_4t) do not depend on the probe spacing. They depend only on the total transmission probability T23 of electron wavefunction between the voltage probes, tip 2 and tip 3 (which are also the current probes in the two-terminal measurement). A remarkable feature of the ballistic transport is that R_4t takes any value between $-R_2t$ and $+R_2t$, meaning that R_4t can be negative by quantum interference effects [21]. At liquid-He temperature, the mean free path of conduction electrons in a $CoSi_2$ film with the thickness of 110 nm becomes ca. 100 nm [27]. Therefore, at low temperatures, we can possibly observe quantum interference effects in resistance at probe spacing we achieved here by using the PtIr-coated CNT tips. The probe spacing dependence of R_4t in the present experiment also excludes observable effects of carrier localization.

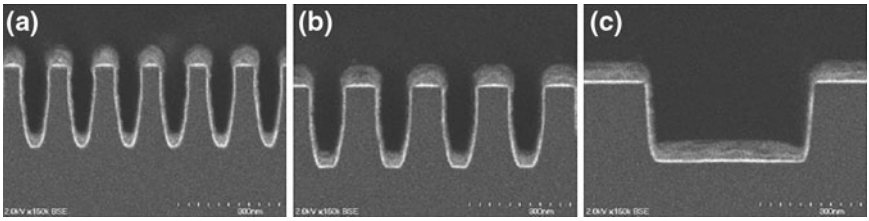

Fig. 6 Cross-sectional SEM image of damascene trenches. The trench widths are **a** 70 nm **b** 100 nm, and **c** 500 nm, respectively [29]

5 Measuring Cu Nanowires

Copper (Cu) wires are now widely used for interconnects in semiconductor devises. But, as the wire width reaches down to the sub-micrometer scale, which is comparable to the mean free path of conduction electrons in the wires, a significant increase in the resistivity has been observed. This is speculated as due to the increased surface and grain boundary scatterings. As the wire width scales down, electrons will undergo reflections more frequently at the surfaces/interfaces, so the collisions with the surfaces/interfaces will become a significant fraction of the total number of collisions. In addition, grain boundaries in polycrystalline wires may act like partially reflecting planes for electron waves, so they also contribute to the increase of resistivity. To investigate these effects directly, the conductivity measurements by the four-tip STM at nanometer scales is very useful [29].

Cu wires having the width between 70 nm and 1 μm were prepared using a Cu/Low-k damascene processes which are now very common in semiconductor industry. Figure 6 shows the cross-sectional SEM images of the damascene structure made in SiO_2 layer. Tantalum (Ta) was used as a barrier metal (BM) in this experiment. Cu damascene lines were formed using conventional Cu process such as seed Cu, electrochemical plating (ECP) Cu for trench filling, and chemical–mechanical polishing. The Cu nanowires are not single-crystalline; they are consisted of small gains. By the electron back-scatter diffraction (EBSD) method, such grains are visualized along the Cu damascene lines [29]. The average grain size was measured to be about 100 nm at 70 nm wide Cu nanowires, which did not change so much with the width, because the grain size is thought to be determined by the height when the width is smaller than the height.

The four-tip STM was used to measure the resistance of individual wires as shown in Fig. 7. By using Pt-coated CNT tips, the probe spacing can be reduced down to the order of several ten nm routinely [23]. When the Pt-coated CNT tips were used, the contact resistance between the tip and sample could not be smaller than 50 kΩ because of its very small contact area. This means that it is impossible to measure conductive materials whose resistance is less than 50 kΩ by the two-point probe method. Only with the four-point probe method, resistances much smaller than the contact resistance (as small as 0.1Ω in the present case) can be measured. Therefore, the combination of the CNT tips and the four-tip STM is very powerful for studies in nanoscale measurements.

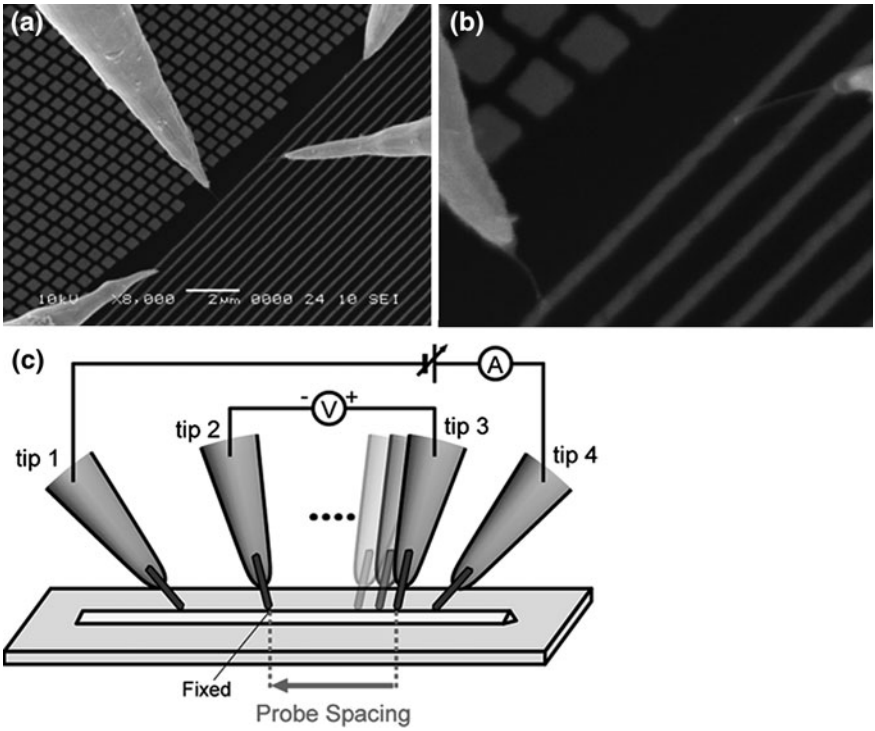

Fig. 7 **a** An SEM image of the Cu wire being contacted with the four probes [29]. **b** The enlargement of the area of rectangle in (**a**). **c** The illustration of the four-terminal I–V measurement

Four-terminal I–V measurements were performed by sweeping the bias voltage between the outer pair of tips and recording the current I and the voltage drop V between the inner pair of tips (Fig. 7c). The probe spacing between the voltage probes was reduced while measuring the I–V characteristics. The two current probes (tip 1 and tip 4) and one of the voltage probes (tip 2) were fixed during the measurements, and only tip 3 was moved between tip 2 and tip 4 (Fig. 7c).

The measured values of four-terminal resistance as a function of the probe spacing between the contact points of the voltage probes on the Cu wires are shown in Figs. 8 and 9. For all of them, the probe spacing dependence of resistance basically showed a linear one-dimensional feature, meaning a diffusive transport. By multiplying the gradient of the fitted straight lines and the cross section of Cu wires (which was estimated from SEM image in Fig. 6), the three-dimensional resistivity was calculated as 4.6, 3.7, and 3.4 Ω cm, for the 70, 50 nm, and 1 μm wide Cu wires, respectively. The resistivity of Cu increased as the line width decreased as shown in Fig. 9b. This result is understood by the Fuchs–Sondheimer theory for the surface-scattering effect and the Mayadas–Shatzkes model for the grain boundary effect [29]. No change in the measured resistance

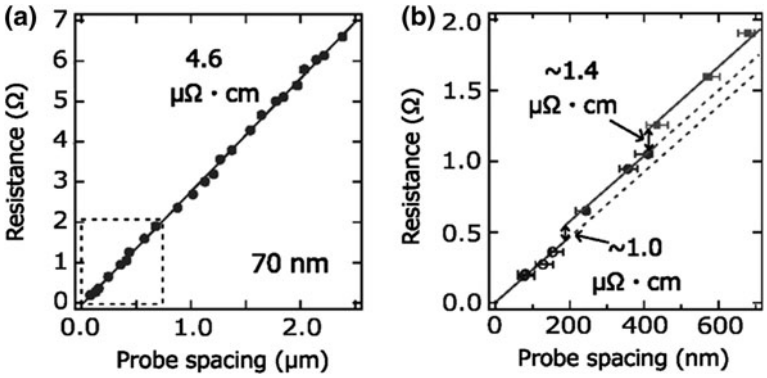

Fig. 8 **a** The measured resistances of the 70 nm wide Cu wire are shown as a function of probe spacing. **b** The enlargement of the area under 600 nm of probe spacing [29]

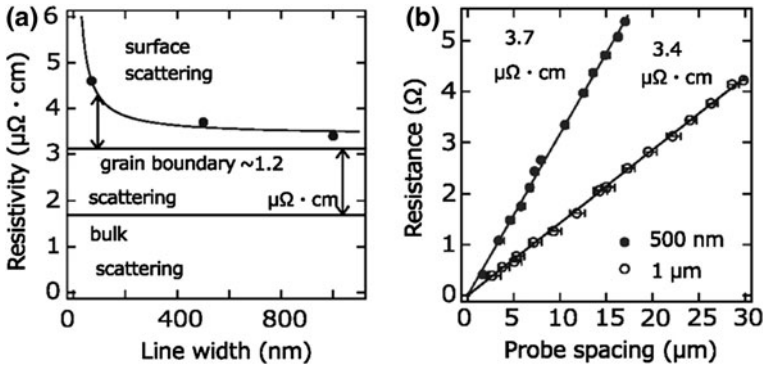

Fig. 9 **a** The measured resistances of Cu wires are shown as a function of probe spacing for the 500 nm and 1 μm wide wires. **b** Plot of the resistivity versus Cu line width [29]. The resistivity coming from the grain boundary scattering is assumed to be constant because the gran size is roughly independent of the line with in our samples

was found in each measurement before and after repeated contacts of CNT tips. It means no significant damage on the sample by the probe contacts.

In this experiment, the probe spacing was reduced to the scale which is comparable with the grain size. Therefore, it can be expected that there will be some change in the resistance when the probe spacing becomes so short that electrons do not undergo grain boundary scattering. This has been indeed observed. Figure 8b shows the enlarged view of the data shown in Fig. 8a for the probe spacing smaller than 600 nm. There is a slight jump in resistance when the probe spacing is shorter than 200 nm. This directly corresponds to the grain boundary scattering where additional resistance occurs at the grain boundary due to the reflection of electron wave there.

6 Concluding Remarks

Electrical measurements using metal-coated CNT tips in the four-tip STM have been demonstrated for the $CoSi_2$ nanowires and Cu damascene wires. Since the apex of CNT tips is around 10 nm and the aspect ratio is so large, it is able to measure the resistance at nanoscale surface areas. The minimum probe spacing in the four-point probe resistance measurement was reduced to a few 10 nm, which is similar or less than the grain size of polycrystalline wires and even the carrier mean free path. The resistance along the wires present here increased linearly with the measured length, meaning classical diffusive transport. But very recently, we have found quasi-ballistic transport in semiconducting $FeSi_2$ nanowires at room temperature where the carrier mean free path is much longer than that of the metallic wires. The details will be reported elsewhere. In the case of Cu damascene wires, the resistivity increased as the wire width decreased. This is due to the surface/interface scattering of carrier. We have evaluated the surface/interface scattering quantitatively to obtain the specularity factor in Fuchs-Sondheimer theory. At the very narrow probe spacing which was comparable to the grain size, the resistance jump due to a single grain boundary was clearly observed. As demonstrated by the measurements presented here, the four-tip STM with CNT tips is a very useful tool for transport physics at nanoscale as well as industrial purposes.

Acknowledgments The present work was done in collaboration with UNISOKU Co., Ltd. in construction of the four-tip STM and Prof. M. Katayama in fabricating CNT tips. It was fully supported by the SENTAN Program of the Japan Science and Technology Agency (JST), and also by Grants-in-Aid for Scientific Research and A3 Foresight Program from the Japanese Society for the Promotion of Science (JSPS).

References

1. Kubo, O., Shingaya, Y., Nakayama, M., Aono, M., Nakayama, T.: Epitaxially grown WOx nanorod probes for sub-100 nm multiple-scanning-probe measurement. Appl. Phys. Lett. **88**, 254101 (2006)
2. Tsukamoto, S., Siu, B., Nakagiri, N.: Twin-probe scanning tunneling microcope. Rev. Sci. Instrum. **62**, 1767 (1991)
3. Okamoto, H., Chen, D. M.: An ultrahigh vacuum dual-tip scanning tunneling microscope operating at 4.2 K. Rev. Sci. Instr. **72**, 4398 (2001)
4. Watanabe, H., Manabe, C., Shigematsu, T., Shimizu, M.: Single molecule DNA device measured with triple-probe atomic force microscope. Appl. Phys. Lett. **78**, 2928 (2001); **79**, 2462 (2001)
5. Lin, X., He, X.B., Yang, T.Z., Guo, W., Shi, D.X., Gao, H.-J., Ma, D.D.D., Lee, S.T., Liu, F., Xie, X.C.: Intrinsic current-voltage properties of nanowires with four-probe scanning tunneling microscopy: A conductance transition of ZnO nanowire. Appl. Phys. Lett. **89**, 043103 (2006)
6. Guise, O., Marbach, H., Yates Jr, J.T., Jung, M.-C., Levy, J.: Development and performance of the nanoworkbench: A four tip STM for conductivity measurements down to submicrometer scales. Rev. Sci. Instr. **76**, 045107 (2005)
7. Ishikawa, M., Yoshimura, M., Ueda, K.: Development of four-probe microscopy for electric conductivity measurement. Jpn. J. Appl. Phys. **44**, 1502 (2005)

8. Takami, K., Akai-Kasaya, M., Saito, A., Aono, M., Kuwahara, Y.: Construction of independently driven double-tip scanning tunneling microscope. Jpn. J. Appl. Phys. **44**, L120 (2005)
9. Grube, H., Harrison, B.C., Jia, J.F., Boland, J.J.: Stability, resolution, and tip–tip imaging by a dual-probe scanning tunneling microscope. Rev. Sci. Instr. **72**, 4388 (2001)
10. Bannani, A., Bobisch, C.A., Möller, R.: Local potentiometry using a multiprobe scanning tunneling microscope. Rev. Sci. Instrum. **79**, 083704 (2008)
11. Omicron Nano Technology GmbH (http://www.omicron.de/), MultiProbe, Inc (http://www.multiprobe.com/), Zyvex Co. (http://www.zyvex.com/)
12. Shiraki, I., Tanabe, F., Hobara, R., Nagao, T., Hasegawa, S.: Independently driven four-tip probes for conductivity measurements in ultlahigh vacuum. Surf. Sci. **493**, 633 (2001)
13. Hasegawa, S., Shiraki, I., Tanabe, F., Hobara, R.: Transport at surface nanostructures measured by four-tip STM. Current Appl. Phys. **2**, 465 (2002)
14. Hobara, R., Nagamura, N., Hasegawa, S., Matsuda, I., Yamamoto, Y., Ishikawa, K., Nagamura, T.: Variable-temperature independently-driven four-tip scanning tunneling microscope. Rev. Sci. Inst. **78**, 053705 (2007)
15. Ikuno, T., Katayama, M., Kishida, M., Kamada, K., Murata, Y., Yasuda, T., Honda, S., Lee, J.-G., Mori, H., Oura, K.: Metal-coated carbon nanotube tip for scanning tunneling microscope. Jpn. J. Appl. Phys. **43**, L644 (2004)
16. Yoshimoto, S., Murata, Y., Hobara, R., Matsuda, I., Kishida, M., Konishi, H., Ikuno, T., Maeda, D., Yasuda, T., Honda, S., Okado, H., Oura, K., Katayama, M., Hasegawa, S.: Electrical characterization of metal-coated carbon-nanotube tips. Jpn. J. Appl. Phys. **44**, L1563 (2005)
17. Konishi, H., Murata, Y., Wongwiriyapan, W., Kishida, M., Tomita, K., Motoyoshi, K., Honda, S., Katayama, M., Yoshimoto, S., Kubo, K., Hobara, R., Matsuda, I., Ha-segawa, S., Yoshimura, M., Lee, J.-G., Mori, H.: High-yield synthesis of conductive carbon nanotube tips for multiprobe scanning tunneling microscope. Rev. Sci. Instr. **78**, 013703 (2007)
18. Kanagawa, T., Hobara, R., Matsuda, I., Tanikawa, T., Natori, A., Hasegawa, S.: Anisotropy in conductance of a quasi-one-dimensional metallic surface state measured by square micro-four-point probe method. Phys. Rev. Lett. **91**, 036805 (2003)
19. Shingaya, Y., et al.: Carbon nanotube tip for scanning tunneling microscopy. Phys. B **323**, 153 (2002)
20. Ishikawa, M., et al.: Simultaneous measurement of topography and contact current by contact mode atomic force microscopy with carbon nanotube probe. Jpn. J. Appl. Phys. **41**, 4908 (2002)
21. Ueda, K., Yoshimura, M., Nagamura, T.: A fabrication method tips for scanning probe microscopes and its apparatus, Japan Patent 2004, No. 3557589
22. Tang, J., Gao, B., Geng, H., Velev, O.D., Qin, L.-C., Zhou, O.: Assembly of ID nanostructures into sub-micrometer diameter fibrils with controlled and variable length by dielectrophoresis. Adv. Mater. **15**, 1352 (2003)
23. Yoshimoto, S., Murata, Y., Hobara, R., Matsuda, I., Kishida, M., Konishi, H., Ikuno, T., Maeda, D., Yasuda, T., Honda, S., Okado, H., Oura, K., Katayama, M., Hasegawa, S.: Four-point probe resistance measurements using ptIr-coated carbon nanotube tips. Nano Lett. **7**, 956 (2007)
24. Murata, Y., Yoshimoto, S., Kishida, M., Maeda, D., Yasuda, T., Ikuno, T., Honda, S., Okado, H., Hobara, R., Matsuda, I., Hasegawa, S., Oura, K., Katayama, M.: Exploiting metal coating of carbon nanotubes for scanning tunneling microscopy probes. Jpn. J. Appl. Phys. **44**, 5336 (2005)
25. He, Z., Smith, D.J., Bennett, P.A.: Endotaxial silicide nanowires. Phys. Rev. Lett. **93**, 256102 (2004)
26. Okino, H., Matsuda, I., Hobara, R., Hosomura, Y., Hasegawa, S., Bennett, P.A.: In situ resistance measurements of epitaxial cobalt silicide nanowires on Si(110). Appl. Phys. Lett. **86**, 233108 (2005)
27. Hensel, J.C., Tung, R.T., Poate, J.M., Unterwald, F.C.: Specular boundary scattering and electrical transport in single-crystal thin films of $CoSi_2$. Phys. Rev. Lett. **54**, 1840 (1985)
28. Allen, P.B., Schulz, W.W.: Bloch-Boltzmann analysis of electron transport in intermetallic compounds - ReO_3, $BaPbO_3$, $CoSi_2$, and Pd_2Si. Phys. Rev. B **47**, 14434 (1993)
29. Kitaoka, Y., Tono, T., Yoshimoto, S., Hirahara, T., Hasegawa, S., Ohba, T.: Direct detection of grain boundary scattering in damascene Cu wires by nanometer-scale four-point probe resistance measurements. Appl. Phys. Lett. **95**, 052110 (2009)